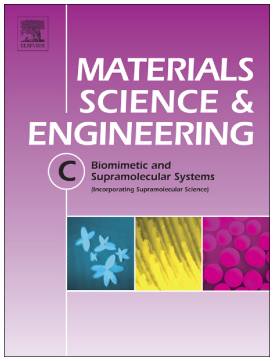

Role of magnesium oxide and strontium oxide as modifiers in silicate-based bioactive glasses: Effects on thermal behaviour, mechanical properties and in-vitro bioactivity

Devis Bellucci, Antonella Sola, Roberta Salvatori, Alexandre Anesi, Luigi Chiarini, Valeria Cannillo

PII: S0928-4931(16)31308-X
DOI: doi: 10.1016/j.msec.2016.11.110
Reference: MSC 7164

To appear in: *Materials Science & Engineering C*

Received date: 13 September 2016
Revised date: 16 November 2016
Accepted date: 23 November 2016

Please cite this article as: Devis Bellucci, Antonella Sola, Roberta Salvatori, Alexandre Anesi, Luigi Chiarini, Valeria Cannillo , Role of magnesium oxide and strontium oxide as modifiers in silicate-based bioactive glasses: Effects on thermal behaviour, mechanical properties and in-vitro bioactivity. The address for the corresponding author was captured as affiliation for all authors. Please check if appropriate. Msc(2016), doi: 10.1016/j.msec.2016.11.110

Role of magnesium oxide and strontium oxide as modifiers in silicate-based bioactive glasses: effects on thermal behaviour, mechanical properties and in-vitro bioactivity.

Devis Bellucci[1*], Antonella Sola[1], Roberta Salvatori[2] , Alexandre Anesi[2], Luigi Chiarini[2] and Valeria Cannillo[1]

[1] Department of Engineering "E. Ferrari", University of Modena and Reggio Emilia, Via P. Vivarelli 10, 41125 Modena, Italy.

[2] Lab. Biomaterials, Department of Medical and Surgical Sciences of Children & Adults, University of Modena and Reggio Emilia, Via Campi 213/A, 41125 Modena, Italy

[*] Corresponding-Author: Dr. D. Bellucci,

Department of Engineering "E. Ferrari", University of Modena and Reggio Emilia, Via P. Vivarelli 10, 41125 Modena, Italy

Telephone: +39-059-2056233; fax: +39-059-2056243; e-mail: devis.bellucci@unimore.it

Abstract

The composition of a CaO-rich silicate bioglass (BG_Ca-Mix, in mol%: 2.3 Na_2O; 2.3 K_2O; 45.6 CaO; 2.6 P_2O_5; 47.2 SiO_2) was modified by replacing a fixed 10 mol% of CaO with MgO or SrO or fifty-fifty MgO-SrO. The thermal behavior of the modified glasses was accurately evaluated via differential thermal analysis (DTA), heating microscopy and direct sintering tests. The presence of MgO and/or SrO didn't interfere with the thermal stability of the parent glass, since all the new glasses remained completely amorphous after sintering (treatment performed at 753 °C for the glass with MgO; at 750 °C with SrO; at 759 °C with MgO and SrO). The sintered samples achieved good mechanical properties, with a Young's modulus ranging between 57.9 ± 6.7 for the MgO-SrO modified

composition and 112.6 ± 8.0 GPa for the MgO-modified one If immersed in a simulated body fluid (SBF), the modified glasses after sintering retained the strong apatite forming ability of the parent glass, in spite of the presence of MgO and/or SrO. Moreover, the sintered glasses, tested with MLO-Y4 osteocytes by means of a multi-parametrical approach, showed a good bioactivity *in vitro*, since neither the glasses nor their extracts caused any negative effect on cell viability or any inhibition on cell growth. The best results were achieved by the MgO-modified glasses, both BGMIX_Mg and BGMIX_MgSr, which were able to exert a strong stimulating effect on the cell growth, thus confirming the beneficial effect of MgO on the glass bioactivity.

Keywords: Bioactive glass; Strontium oxide; Magnesium oxide; Bioactivity; Bone regeneration; Cell culture.

1. Introduction

Bioactive glasses are nowadays well-established biomaterials for orthopaedic applications and bone tissue regeneration. The first scientific evidence of the bone-bonding ability of bioactive glasses dates back to the second half of the 20th century, thanks to the research activity carried out by Prof. Hench and co-workers. In 1969, Hench and colleagues formulated indeed a new specific glass in the Na_2O-CaO-P_2O_5-SiO_2 system and implanted it into the femurs of rats. The *in vivo* tests proved that the glass was able to bond to bone directly, without the non-adherent fibrous capsule that typically grows up as a result of foreign-body response [1]. The name of the new glass, 45S5 Bioglass®, reflected its composition, which included 45 wt% of SiO_2 as network former. Na_2O and CaO, 24.5 wt% each, were added as glass modifiers, whereas 6 wt% of P_2O_5 was introduced to simulate the Ca/P ratio of hydroxyapatite ($Ca_5(PO_4)_3(OH)$, "HA" in the following), which is the main mineral component of bone [2]. Subsequent investigations proved that 45S5 Bioglass® and other specific silicate-based bioactive glasses are able to bond not only to bone, but also to soft tissues; moreover they are able to stimulate angiogenesis and

osteoblast turnover [3, 4]. On account of its excellent bioactivity, 45S5 Bioglass® is nowadays used in several clinical applications. In 2009, the same year of the 40th anniversary of the first discovery of the glass, two sale records were set, since both the one millionth dose of bone graft product (NovaBone and Perioglas) and the one millionth tube of tooth paste containing 45S5 particulate (NovaMin) were sold [5].

However, the original glass formulation suffers from some drawbacks. In more detail, thermal processing of 45S5 Bioglass® and related glasses, in order to obtain sintered materials, scaffolds and coatings, is known to promote a wide devitrification. The optimal temperature range to sinter 45S5 Bioglass® (550 °C up to 610 °C) is indeed very close to its crystallization temperature (about 610 °C) and high temperature treatments are further required to complete the densification thanks to a second sintering step, between around 950 °C and 1100 °C. The crystallization may improve the mechanical properties of the final material, but it inhibits sintering, since it reduces the volume fraction of glass for viscous flow sintering. Moreover, crystallization may also affect the glass bioactivity, since, according to the available literature, the new crystal phases are less reactive and hence less bioactive than the amorphous counterpart. It is reported that devitrification of 45S5 Bioglass® reduces the rate of conversion to HA , and the ability for a given bioactive glass to stimulate tissue regeneration at a cellular level is related to its rate of dissolution in a physiological environment and to the conversion to HA [6–11]. Finally, a partial crystallization can lead to instability, since the remaining amorphous areas degrade preferentially *in vivo* [12] and this fact may cause the implant to fail due to long-term instability of interphase boundaries.

Over the years, various attempts have been made to improve the sinterability of the glass through an appropriate change in composition [13, 14]. For example, increasing the CaO-to-Na_2O ratio proved to be a valuable way to raise the crystallization temperature and hence to promote the sintering process, which could be completed at 800 °C instead of about 950-1100 °C, as usually observed for 45S5 Bioglass® [15, 16]. Additional investigations showed that the thermal behaviour of the glass could be modified further by partially or completely substituting the residual Na_2O with K_2O [17–19]. The modified

formulations did not impair the biocompatibility of the glass, but they greatly favoured the fabrication of glass-based coatings, composites and scaffolds [20–22].

However, it is worth noting that the composition of a bioactive glass exerts a prominent effect not only on its thermal and mechanical behaviour, but also on its biological role. For example, it is known that the addition of as little as 3 wt% Al_2O_3 to 45S5 Bioglass® is enough to restrain the bone-bonding ability of the glass [2, 13]. As a matter of fact, the ionic dissolution products of bioactive glasses and related glass-ceramics are expected to play a specific role in relation to both osteogenesis and angiogenesis. As a consequence, the addition of specific elements such as magnesium, zinc, fluorine, copper, strontium and boron can be used to modulate the biological, as well as the mechanical performance of materials for bone replacement [23]. In particular, magnesium (Mg) is essential for numerous biological processes in the human body and it is one of the most important ions associated with biological apatites: for example, dentin and bone are composed by 1.11 wt% and 0.47 wt% of Mg, respectively [24]. Mg is known to stimulate osteoblast proliferation, differentiation and bone mineralization ability [25]; it was also reported that Mg regulates active calcium transport and activates phagocytosis, while in calcified tissues it is involved in the calcification process [23, 26]. Mg deficiency may be related to reduced osteoclastic and osteoblastic activities, leading to bone fragility and/or decreased bone growth [25, 27]. A comprehensive review describing the role of Mg in bone tissue engineering and the biological properties of Mg-containing bioactive glasses can be found in [28].

The importance of strontium (Sr) in the human body makes it a very interesting element as a component/dopant of bioactive glasses [23]. Strontium incorporation in bioactive glasses can accelerate bone-healing processes, stimulate osteoblasts and inhibit osteoclasts *in vitro* [29, 30]; this means that the addition of Sr can be used to increase osteogenesis *in vivo* and, at the same time, to reduce bone resorption. For this reason Sr is considered a promising agent for treating osteoporosis [23] and it has been employed as the active ingredient of antiosteoporotic drugs such as strontium ranelate [31]. The positive effects of magnesium and strontium in terms of bone generation are witnessed by their diffused presence as

dopants in hydroxyapatite and other calcium-phosphate based systems [32, 33]. On the other hand, in the literature there is a lack of specific investigations focused on bioactive glasses containing both Mg and Sr, in order to study the combined effects of such ions on the properties of the final product.

The main target of the present contribution is to combine the favourable thermal behaviour of Ca-rich silicate glasses with the improved biological outcomes of MgO- and SrO-modified glasses, where MgO and SrO were preferred to other oxides on account of their documented benefits to bone generation [23]. With this aim, the parent glass (BG_Ca-Mix, in mol%: 2.3 Na_2O; 2.3 K_2O; 45.6 CaO; 2.6 P_2O_5; 47.2 SiO_2) [17] was modified by replacing a fixed 10 mol% of CaO with the same amount of MgO (BGMIX_Mg) or SrO (BGMIX_Sr) or fifty-fifty MgO-SrO (BGMIX_MgSr). The combined substitution of 10 mol% CaO with fifty-fifty MgO-SrO specifically aims to reveal any possible interaction between the two modifiers, an issue scarcely investigated in the literature. The new compositions are reported in Table 1. The effect of the addition of MgO and/or SrO was carefully analysed in terms of thermal behaviour, mechanical properties and *in vitro* bioactivity.

2. Materials and Methods

2.1 Preparation of glass powders

The glasses (BG_Ca-Mix, BGMIX_Mg, BGMIX_Sr, BGMIX_MgSr) were produced by a melt-quenching route as described previously [14, 17, 19]. Briefly, the commercial raw powders (SiO_2, $Ca_3(PO_4)_2$, $CaCO_3$, Na_2CO_3, K_2CO_3, $(MgCO_3)_4\ Mg(OH)_2\ 5H_2O$, $SrCO_3$, all reagent grade - Carlo Erba Reagenti, Italy) were weighted, mixed for 2 h in a laboratory shaker (M63a4 – Motori Elettrici Carpanelli, Bologna, Italy) and then melted in a Pt crucible in air. The following thermal cycle was performed: from room temperature to 1100 °C at 10 °C/min; a decarbonation step at 1100 °C for 1 h; from 1100 °C to 1450 °C at 10 °C/min; 1 h at 1450 °C to obtain a homogeneous melt. The molten glass was quickly

quenched in room-temperature water to obtain a frit, which was subsequently dried overnight at 110 °C. The frit was then ground for 20 minutes in dry conditions in a porcelain jar and sieved to produce a powder with a final grain size lower than 67 μm.

2.2 Analysis of thermal behaviour

The glasses were characterized by Differential Thermal Analysis (DTA) using a Netzsch Differential Thermal Analyzer DSC 404 (NETZSCH-Gerätebau GmbH, Selb, Germany). 30 mg of each glass powder were put in an inert Pt crucible and heated from room temperature to 1200 °C, at a constant heating rate of 10 °C/min. The glass transition temperature (T_g), the onset crystallization temperature (T_{c_onset}) and the peak crystallization temperature (T_c) were then defined for each sample from the corresponding DTA graph. Heating microscopy (Misura 3.32; Expert System Solutions, Modena, Italy) was performed on the glass powders from room temperature to 1300 °C at 10 °C/min in order to determine the sintering temperature (T_s) and melting one (T_m).
The sintering attitude of the MgO and/or SrO modified glasses was estimated by the sinterability parameter, S_C, defined according to the equation [34]:

$$S_C = T_{c\_onset} - T_s \quad (1)$$

2.3 Sintering

BGMIX_Mg, BGMIX_Sr, BGMIX_MgSr powders were wetted with acetone and then pressed in order to obtain 15 mm-diameter disks (green bodies). The green bodies were sintered for 3 h at the final temperatures T_s identified by the heating microscopy analysis as reported in Table 2 (heating rate of 10 °C/min from room temperature to T_s). In particular, the densification of the green bodies was monitored by evaluating their volume shrinkage $\Delta_\%$ after the thermal treatment. $\Delta_\%$ was calculated according to the equation

$$\Delta_\% = \frac{d_0 - d_e}{d_0} \cdot 100 \quad (2)$$

where d_0 and d_e are the nominal diameter of the press (15 mm) and the measured diameter of the sample after heat treatment, respectively. In order to evaluate the effect of crystallization, a second set of samples was treated at T = 1000 °C (i.e. > T_c) for 3 h; moreover, an additional group of BGMIX_Mg samples was treated at T_c = 876 °C for 3 h. For comparison purposes, especially in terms of biological responsiveness, in-lab produced BG_Ca-Mix powders and commercially available Bioglass® 45S5 powders (MO-SCI Corporation, Rolla, MO, USA) were processed in the same way. BG_Ca-Mix and 45S5 samples were indeed pressed and subsequently sintered for 3 h at T_s = 800 °C and T_s = 1050 °C, respectively, according to the findings reported in previous works [17, 18, 35].

2.4 Microstructural and mechanical characterization

After the thermal treatment, the samples were investigated by means of X-ray diffraction (XRD) employing a Panalytical X'pertPRO diffractometer (Panalytical, Almelo, The Netherlands) equipped with a copper (Cu Kα) X-ray source. The samples were scanned between 2θ = 10° and 2θ = 70° with a step size of 2θ = 0.02°. The microstructure of the samples was observed in an Environmental Scanning Electron Microscope (ESEM Quanta 2000, FEI Co., Eindhoven, The Netherland) before and after immersion in a Simulated Body Fluid solution (SBF, see following sections). The ESEM was employed in low-vacuum conditions (~0.5 Torr). X-ray energy dispersion spectroscopy (EDS) (Inca, Oxford Instruments, UK) was used to perform qualitative compositional analyses.
The sintered samples were cut and the cross sections were ground and polished according to a standard ceramographic procedure [36]. In order to determine the Vickers hardness of the sintered glasses, Vickers micro-indentation tests (Wolpert Group, Micro-Vickers Hardness Tester digital auto turret, Mod. 402MVD) were performed on the polished cross-sections. A maximum load of 100 g_f was applied for 15 s and at least 15 indents (clear and crack-free) were considered and analysed for each material [37].

As for the local elastic modulus, a depth-sensing micro-indentation technique was applied, operating with an Open-Platform instrument (CSM Instruments, Peseux, Switzerland) equipped with a Vickers indenter tip. For each indentation, the applied load and the corresponding penetration depth were measured and the elastic modulus was calculated from the unloading part of the load–depth graph by means of the Oliver-Pharr method [38]. For each material, at least fifteen indentations were performed on the polished cross section using standard parameters: maximum applied load: 1 N; loading/unloading rate: 1.5 N/min; loading time at maximum load: 15 s.

2.5 Investigation of the in vitro bioactivity

The bioactivity of the sintered samples was investigated by soaking them in 25 ml of Simulated Body Fluid solution (SBF), according to the protocol originally developed by Kokubo et al [39]. The samples were stored in plastic flasks and maintained at 37 °C; the solution was periodically refreshed every 48 hours to simulate the fluid circulation in the body. The samples were removed from the SBF after 1, 3, 7 and 14 days, rinsed with distilled water and dried at room temperature. The formation of a HA layer on the samples' surface was evaluated by means of ESEM, XRD and micro-Raman spectroscopy. For the micro-Raman analysis, a Jobin-Yvon Raman Microscope spectrometer (Horiba Jobin-Yvon, Villeneuve D'Aseq, France) was used, with a 632.8 nm He-Ne diode laser source focused through a 100x objective.

2.6 Biological tests

MLO-Y4 (murine long bone osteocyte Y4 cell line) cells were used in order to investigate the biocompatibility of the prepared glasses *in vitro*. In particular, the materials' cytotoxicity was evaluated according to International Standards 10993–5 and 10993–12 [40, 41]. Neutral Red (NR) uptake, tetrazolium salt XTT (2,3-bis(2-methoxy-4-nitro-5-sulfophenyl)-5-[(phenylamino) carbonyl]-2H-tetrazolium hydroxide) and

Bromodeoxyuridine (BrdU) assays were employed to investigate cell viability and proliferation. The cytotoxicity of the sintered glasses was evaluated through direct and indirect contact, in order to investigate possible cytotoxic effects of the glasses' eluates. The samples (10 mm diameter sintered discs) were sterilized in ethylene oxide before biological tests.

2.6.1. Culture of MLO-Y4 cells

MLO-Y4 cells were grown as a confluent monolayer in Dulbecco's modified Eagle's medium (DMEM) containing L-Glutamine 2mM, 1 mM sodium pyruvate, pen-streptomycin and 10% (v/v) FBS (fetal bovine serum – Invitrogen). The cells were cultured in 6-well plates for NR uptake assay (i.e. direct contact with the samples) and in 96-well plates containing the glasses' extracts for XTT and BrdU tests (i.e. indirect contact tests, see following paragraphs). The cells were maintained in an incubator at 37°C ± 1°C, 5.0 % ± 1 % CO_2/air and 90 % ± 5 % humidity.

2.6.2. Preparation of the glasses' eluates

The samples were treated in centrifuge tubes, 6 cm^2/ml area, each containing DMEM. DMEM supplemented with 0.45% (v/v) of phenol solution, a cytotoxic agent, was employed as positive reference (CTRL +), while DMEM only was used as negative control (CTRL-). The flasks were incubated at 37°C for 5 days. Finally, the pH was measured and the eluates were filtered using a 0.22 μm filter.

2.6.3. NR uptake and morphological evaluations

MLO-Y4 cells were cultured in 6-well plates in direct contact with the sintered glasses, at 37°C ± 1°C, 5.0 % ± 1 % CO_2/air and 90 % ± 5 % humidity. After 24h of incubation, the morphology of the cells was observed by means of an optical microscope (Nikon TMF,

Japan). Subsequently, the culture medium was removed and 250 µl of NR solution was added to each well. The plates were incubated for 3 h at 37°C ± 1°C, 5.0 % ± 1 % CO_2/air and 90 % ± 5 % humidity, then the NR solution was removed and the cells were washed to remove the excess NR solution. 100 µl of extraction solution (freshly prepared ethanol/acetic acid) was added to each well and the plate was incubated at room temperature for 20 min in order to extract NR from the cells. The test was repeated in triplicate for each glass. Finally, the amount of dye concentrated within the cells was evaluated by measuring the absorbance at 540 nm of all wells, including the CTRL+ and CTRL- ones, by means of a spectrophotometer (Multiscan RC by Thermolab system, Finland).

2.6.4. XTT test

Cells were grown in 96-well plates and then incubated at 37°C ± 1°C, 5.0 % ± 1 % CO_2/air and 90 % ± 5 % humidity with the eluates of the samples for 24 h. Subsequently, XTT labelling solution (Cell Proliferation Kit II (XTT) Roche diagnostics, USA) was added to each well (final concentration 0.3 mg/ml). After 4 h at the same incubation conditions, XTT is reduced to a water-soluble product, i.e. an orange formazan dye, whose amount is proportional to the number of living cells. To quantify the amount of the newly synthesized formazan, the absorbance of all wells was measured at 490 nm.

2.6.5. Bromodeoxyuridine (BrdU) test

MLO-Y4 cells were cultured in 96-well multi plates at a concentration of $7x10^3$ cells per well. The extracts of the samples were added directly to the medium. After 24 h exposure to the samples' eluates, 10 µl/well of BrdU labeling solution (Cell Proliferation ELISA, BrdU , Roche, Germany) was added and the plates were incubated for 5 h at 37°C ± 1°C, 5.0 % ± 1 % CO_2/air and 90 % ± 5 % humidity. During this period, BrdU is incorporated by the cycling cells in place of thymidine into their newly synthesized DNA. The labeling

medium was then removed, 200 µl/well of FixDenat solution (Cell Proliferation ELISA, BrdU, Roche, Germany) was added and the plates were incubated for 30 minutes at room temperature, in order to fix the cells and to denature DNA in a single step. After removing FixDenat, the anti-BrdU-POD antibody, i.e. an antibody conjugated to peroxidise, was added (100 µl/well). The anti-BrdU-POD antibody binds to the BrdU incorporated into the newly synthesized cellular DNA. After 90 min incubation at room temperature, the antibody conjugate was removed, the wells were rinsed with washing solution [washing buffer (phosphate-buffered saline) 1:10 with double distilled water; Roche, Germany], 100 µl/well of substrate solution (tetramethyl-benzidine 100 ml, ready-to-use; Roche, Germany) was added and the plates were further incubated for 15 min. Finally, the absorbance of the samples was measured at a wavelength of 370 nm. The intensity of the signal is correlated to the amount of the newly synthesized DNA, i.e. to the number of proliferating cells.

2.6.6. Statistical analyses

One-way variance analysis (ANOVA) was employed to statistically treat the results, which are expressed as the mean ± standard deviation. Statistical differences among groups ($p < 0.05$) were established based on a t-test analysis, in which a two-population comparison was considered.

3. Results and Discussion

3.1 Thermal behaviour, sinterability and microstructural characterization

The results of the DTA investigations performed on the glasses are presented in Figure 1. Independently of the glass composition, the curves are characterized by (1) a change in the baseline between 650°C and 680°C, when the glasses undergo a glass transition, and (2) a sharp exothermal peak between 860°C and 885°C, which is associated to the glass

crystallization. While the BGMIX_Sr and BGMIX_MgSr DTA traces show similar trends, the BGMIX_Mg curve presents a second broad exothermal peak at higher temperature (960°C÷980°C), which could be ascribed to a further crystallization process. The characteristic temperatures of the glasses extrapolated by the DTA are listed in Table 2, together with the sintering (T_s) and the melting (T_m) temperatures defined via heating microscopy.

The values in Table 2 indicate that the glass transition temperature T_g of the modified glasses is lower than that of the original BG_Ca-Mix glass, while the trend is less clear for the crystallization temperature, since the peak crystallization temperature (T_c) is comparable for all the glasses, whereas the onset crystallization temperature T_{c_onset} is lower for the modified glasses than for the parent one. As far as the effect of Sr is concerned, a general decrease in T_g with increasing SrO addition was reported in [42], although a direct comparison is difficult because the glass composition employed by Lotfibakhshaiesh et al [42] (i.e. a glass belonging to the Na_2O-K_2O-MgO-ZnO-CaO-SiO_2-P_2O_5 system) strongly differs from the ones discussed in the present work. According to Lotfibakhshaiesh et al, the decrease in T_g of the strontium-modified systems is ascribable to an expansion of their glass network with increasing substitution of Sr for Ca. In fact, the ionic radius of Sr ions is larger than that of Ca ions and therefore non-bridging oxygens are less attracted. This hypothesis was also confirmed by the XRD investigation performed on the glasses [42], which reported a shift towards smaller 2θ values of the maximum of the amorphous halo, which means larger interplanar spacing. Fredholm et al. reported similar conclusions, i.e. an increase in molar volume of the samples, in their study on strontium substituted bioactive glasses [43, 44]. A weaker glass network is also likely to promote the viscous flow, thus resulting in a more efficient sintering.

As to the effect of Mg, several investigations have reported a decrease in T_g with increasing amounts of MgO in silicate glasses [26, 45]. This effect may be explained by the formation of new Si–O–Mg bonds, which are characterized by a lower average bond strength with respect to the original Si–O–Si bonds. In more detail, if the effect of the substitution of MgO for CaO is considered, a pioneering work by Swift et al. analyzed a series of glasses

based on the ternary composition: 16% Na_2O, 10% CaO, 74% SiO_2, where CaO was replaced in 2 wt% steps by MgO. The Authors proved that, up to 6 % MgO, the stability of the glasses increased, since the liquidus temperature decreased progressively and the crystallization rates decreased correspondingly. However, a further replacement of CaO by MgO had the opposite result and the stability of the glass decreased [46]. A progressive increase in T_c as a result of the replacement of CaO by MgO is frequently reported in the literature for silicate based glasses, which means that MgO would exert an inhibitory effect on crystallization [47, 48]. However, it should be stressed that, in general, the role played by MgO in silicate glasses has not been completely clarified yet. In fact it has been reported that MgO (at least up to a certain compositional limit) acts as an intermediate oxide [26, 49], while other investigations suggest that MgO mainly behaves as a glass network modifier [50]. Both the Mg-containing glasses developed in the present work, i.e. BGMIX_Mg and BGMIX_MgSr, are characterized by a T_c rather similar to that of the unmodified parent glass, even if T_{c_onset} is slightly lower than that of the unmodified BG_Ca-Mix (Table 2). Besides the aforementioned ambiguous role of MgO in silicate glasses, in the case of BGMIX_MgSr this fact my be explained in terms of two competing mechanisms which counterbalance each other: on the one hand, the possible inhibitory effect of MgO on crystallization; on the other hand, a weaker glass network caused by the presence of SrO (see previous paragraphs).

To conclude, the effect of the partial substitution of CaO with MgO and/or SrO on the thermal behaviour of the glasses cannot be generalized, since two opposing factors are involved: (1) an increase in the entropy of mixing, which is expected to promote the disordered glass state, thus retarding the crystallization process; (2) a weaker glass network, by which the crystallization would be promoted. As a consequence, the thermal behavior is governed both by the MgO/SrO ratio and by the specific glass composition.

The sintering temperature (T_s) identified by heating microscopy is also reported in Table 2. Preliminary sintering tests were carried out to define adequate sintering conditions for each glass composition. The sintering attitude of the MgO and/or SrO modified glasses was estimated by measuring their volume shrinkage for different sintering conditions and

by calculating a specific sinterability parameter S_C (see Eq. 1) [34, 51, 52]. From a physical point of view, the sinterability parameter S_C of a glass is representative of its sintering ability vs. its crystallization trend. In more detail, if $T_{c\_onset} < T_s$ and hence $S_C < 0$, the glass crystallizes before sintering, which is expected to result in limited densification; vice versa, if $T_{c\_onset} > T_s$ and hence $S_C > 0$, sintering occurs prior to crystallization and hence a good densification should be achieved [34]. Moreover, as a general trend, the greater is the value of S_c, the more independent are the kinetics of sintering and crystallization, which is likely to promote the sintering and compaction process of the glass [34]. On account of the results of the DTA and the heating microscopy reported in Table 2, it is possible to calculate S_C = 78 °C for the original BG_Ca-Mix glass, S_C = 79 °C for BGMIX_Mg, S_C = 88 °C for BGMIX_Sr and S_C = 82 °C for BGMIX_MgSr. The sinterability parameter is therefore greater than zero for all the glasses, with high values that suggest a strong attitude to sinter. This fact is further confirmed by the remarkably strong volume shrinkage associated with sintering (Table 2). This is indicative of the achievement of well-sintered glasses for all the compositions considered in the present contribution, independently of the specific modifier oxide introduced, MgO and/or SrO.

As an alternative to the previous sinterability parameter, the Hrubÿ parameter provides a first-hand idea of the stability of the glass against crystallization on heating and, vice versa, on its vitrifiability on cooling [53]. The Hrubÿ parameter K_H is defined as

$$K_H = \frac{T_{c\_onset} - T_g}{T_m - T_{c\_onset}} \quad (3)$$

where T_{c_onset}, T_g and T_m are the onset crystallization (on heating), the glass transition and the melting temperatures, respectively [53].

Again, introducing the values for T_{c_onset}, T_g and T_m as reported in Table 2, it is possible to calculate K_H = 0.29 for the original BG_Ca-Mix glass, K_H = 0.45 for BGMIX_Mg, K_H = 0.37 for BGMIX_Sr and K_H = 0.46 for BGMIX_MgSr. The obtained K_H values are indicative of the increased stability against crystallization of the modified glasses, especially those containing MgO, with respect to the parent glass. The very limited tendency to crystallize

of the modified glasses was confirmed by the XRD performed on the sintered glasses, which remained indeed completely amorphous (data not shown).

The cross section of the sintered glasses are reported in Figure 2. All the samples are adequately consolidated and possess a dense microstructure, as proved by the shrinkage data (Table 2). This fact confirms the effectiveness of the sintering process which occurs in the investigated glasses. Some fine residual porosity can be observed in the cross sections for all the samples, but it has been widely reported in the literature that the presence of micro-porosity in the implant is not adverse from a biological point of view, because it can favour the osteointegration process [54, 55].

In order to characterize further the thermal behaviour of the glasses, a set of samples was treated at higher temperature, i.e. 1000 °C, which is above T_c for all the glass compositions (in particular, for BGMIX_Mg it is above both crystallization temperatures). The XRD spectra, which refer to the samples sintered at 1000 °C for three hours, are reported in Figure 3. All the glasses showed the formation of $CaSiO_3$, as previously observed for the parent glass BG_Ca-Mix [18, 52]. Several investigations in the literature report that calcium silicate ceramics belonging to the $CaSiO_3$ family have excellent bioactivity and biocompatibility [56–58]. Besides $CaSiO_3$, other specific crystalline phases were observed for each glass composition (see Figure 3). However, the attribution of these secondary phases was difficult due to peak overlapping. As an additional analysis, the BGMIX_Mg glass was also fired at T_c (= 876°C) for three hours. As a matter of fact, since the DTA curve of BGMIX_Mg (Figure 1) was characterized by a first crystallization temperature at T_c = 876 °C and by a second broad crystallization peak between 960 °C and 980 °C, some differences might occur between the crystallization outcome of the BGMIX_Mg sample treated at T_c (= 876°C) and that obtained at T = 1000°C. The diffractogram acquired on the BGMIX_Mg sample fired at 876 °C is reported in the same Figure 3 for comparison purposes. It is worth noting that, even if they refer to two different temperature ranges, the two spectra associated to BGMIX_Mg, at 876 °C and at 1000°C, look qualitatively similar, being characterized by the peaks of $CaSiO_3$ (though with different ICDD codes)

and $MgSiO_3$. The XRD peaks of the sample sintered at higher temperature are sharper, thus indicating a more extensive crystallization.

3.2 Mechanical characterization

As shown in Table 2, the Vickers hardness of the sintered glasses ranges between 448.4 ± 93.8 HV for BGMIX_Mg and 485.2 ± 28.0 HV for BGMIX_Sr. However, due to the scattering of the acquired data, it is not possible to draw a significant ranking among the glasses under exam. In a previous contribution, working under the same experimental conditions, a value of 564 ± 47 HV was found for the Vickers hardness of the sintered BG_Ca-Mix parent glass [18], which shows that the substitution of some CaO with the same amount of MgO and/or SrO has a lowering effect on the hardness of the sintered glasses, even if, in principle, the bond strength pattern varies as MgO > CaO > SrO > BaO [59]. This is probably the result of the complicated interactions occurring among multiple modifier oxides.

As reported in the same Table 2, the elastic modulus varies in the sequence BGMIX_Mg > BGMIX_Sr > BGMIX_MgSr. The trend outlined for the elastic modulus matches well the results of volume shrinkage, since the shrinkage, too, varies in the sequence BGMIX_Mg > BGMIX_Sr > BGMIX_MgSr. As a matter of fact, the presence of residual pores deeply influences the mechanical properties of sintered ceramic materials [60]. In a previous paper, both 45S5 Bioglass® powders and BG_Ca-Mix ones were sintered by means of the Spark Plasma Sintering (SPS) technique. According to the specific processing conditions, the elastic modulus, measured by means of the same depth-sensing Vickers micro-indentation procedure applied here, varied between 66 GPa and 82 GPa for 45S5 Bioglass® and between 65 GPa and 122 GPa for BG_Ca-Mix [61]. The elastic modulus of the new MgO and/or SrO modified glasses are therefore comparable to those of the gold-standard 45S5 Bioglass® and the BG_Ca-Mix parent glass, even if the former were sintered following a conventional thermal treatment, whereas the latter were produced with the SPS technique. Only the elastic modulus of the BGMIX_MgSr sintered glass is slightly lower,

but it should be kept in mind that the present contribution is a starting point, and further improvements to the sintering process and related mechanical properties are expected as a result of appropriate changes in the sintering times and, most of all, in the granulometric distribution of the initial powders.

3.3 In vitro bioactivity

According to the picture proposed by Larry Hench and co-workers [2], bioactive glasses chemically bond to bone through the formation of a surface film of hydroxycarbonate apatite (HCA), which mimics the mineral component of bone, i.e. the biological apatite. HCA is able to support new bone tissue growth along the implant at the interface between bone and the implant itself. This property is called osteoconductivity [62]. The first five stages of the osteointegration process, which usually finish by the initial 24 hours, imply the release of soluble ionic species from the glass and the subsequent development of a bi-layer deposit composed of hydrated silica (silica gel) and polycrystalline HCA on the surface of the implant. The following six stages require the intervention of growth factors and macrophages, the attachment, differentiation and proliferation of osteoblasts, and, to conclude, the generation and crystallization of the bone matrix [63]. The development of HCA highly depends on the glass composition, type (i.e. sol-gel vs melt) and morphology (pellets, powders, scaffolds, fibres, etc). At the beginning of the 90's, Kokubo et al. proposed to reproduce *in vitro* in SBF the *in vivo* HCA formation on the surface of a bioactive material [64]. Today the protocol developed by Kokubo and Takadama [39] is a widely diffused tool to preliminary investigate the bioactivity of new materials, although some criticisms have been expressed, in particular because (1) SBF tests look too simplistic to simulate the complexity of a dynamic biological environment, and (2) they may lead to false negative and false positive results [65].

Previous investigations demonstrated that the BG_Ca-Mix parent glass, both produced by melt quenching and by sol-gel method, showed a high *in vitro* bioactivity after sintering [18, 66]. Figure 4 shows the surface of the new sintered glass samples after soaking in SBF for increasing times; BGMIX_Mg was considered as a representative example. After 1 day

all the glasses have already started their dissolution and it is possible to observe the local formation of some globular deposits. For short immersion times, BGMIX_Mg seems to be the most bioactive composition; in particular, its surface is covered by white aggregates with the typical morphology of HA already after 3 days in SBF. A progressive increase in the amount of HA precipitation with increasing incubation time was observed for all the samples; after 7 and 14 days the surface of the sintered glasses looked indeed rather similar, being completely covered by HA. Apart from local fluctuations, the EDS analysis on the white aggregates measured a Ca/P ratio of about 1.7 (data not shown). This value is comparable to that of stoichiometric apatite (~1.67) [67]. The identification of the precipitates as HCA was confirmed by XRD and Raman analysis. Again, as a representative example, Figure 5 shows the XRD spectra of a BGMIX_Mg sample soaked in SBF for increasing times (for comparison purposes, the spectrum of the sintered BGMIX_Mg sample, not immersed in SBF, is included as well); since the results for BGMIX_Sr and BGMIX_MgSr were similar to the BGMIX_Mg ones, they are not presented for the sake of brevity. Already after one day of immersion, a silica gel film forms on the surface of BGMIX_Mg. This fact is proved by the broad halo in the range 2θ = 20–25° of the spectrum. After three days in SBF, the first peaks ascribable to HA can be observed (2θ = 25–26° and 2θ = 31–33°). The peaks of HA become more clear with increasing soaking times, as the silica gel film is progressively covered by the HA aggregates. After 2 weeks in SBF the XRD of the sintered glasses are rather similar, regardless of the specific composition. All the diffractograms are characterized by HA peaks, detectable but broad due to the presence of structural defects and the microcrystalline nature of the precipitated apatite [68]. After 14 days in SBF, the halo related to the silica gel is less visible in the BGMIX_Mg diffractogram than in the BGMIX_Sr and BGMIX_MgSr ones. This fact can be explained in terms of a thicker HA layer which forms on the BGMIX_Mg glass, which is therefore the most bioactive composition according to the findings of the ESEM investigation.

The formation of HA and its chemical nature were investigated further by means of Raman spectroscopy, which is an useful tool to study the precipitation of apatite, as the

Raman peaks associated to the vibration of the P–O group are particularly intense. Moreover, it is possible to identify if the apatite is carbonated, thanks to the Raman response of the C–O groups. The Raman spectra acquired on the globular aggregates that grew on the BGMIX_Mg surface for increasing soaking times are presented in Figure 6. Analogous results were obtained for BGMIX_Sr and BGMIX_MgSr (data not reported for brevity). It is possible to observe the typical Raman signals ascribable to apatite, i.e. two peaks at about 590 cm^{-1} and 430 cm^{-1}, together with a strong sharp peak at 960 cm^{-1} [69-71]. The peak at about 1070 cm^{-1}, which is related to the stretching of C–O groups, confirms that the apatite formed on the sample surface is carbonated [72].

3.4 Biological tests

The biological tests were performed on the BGMIX_Mg, BGMIX_Sr and BGMIX_MgSr sintered samples. As previously mentioned, two terms of comparison were also considered, namely (i) the BG_Ca-Mix (= parent glass) powders, which were pressed and sintered for 3 hours at T_s = 800 °C; and (ii) the commercially available Bioglass® 45S5 powders, which were pressed and sintered for 3 hours at T_s = 1050 °C [17, 18, 35]. It is worth noting that all the biological tests were focused on sintered samples because the new glasses were formulated specifically to facilitate thermal processing, in view to fabricate scaffolds and other sintered devices.

As previously mentioned, even if soaking in SBF is commonly recognized as a simple and inexpensive way to investigate the apatite forming ability of new materials, several concerns exist about the real significance of this experimental approach, since SBF, being a solution which mimics the acellular and protein-free component of plasma, is unable to reproduce the dynamic physiological environment of the human body and its delicate equilibrium of trace elements [73, 74]. Moreover, various false-positive and false-negative results have been described in the literature [75-78]. Besides this, it has been argued that the apatite-forming ability *in vitro* does not automatically imply the bioactivity *in vivo* [65, 79].

For these reasons, the cytotoxicity of the sintered glasses was tested with respect to MLO-Y4, which is an osteocite-like immortalized cell line isolated from murine long bones, whose properties reproduce those of primary osteocytes [80-83].

As shown in Figure 7, after 24 h of direct contact with the sintered glasses, no relevant effects could be detected on the behaviour of the MLO-Y4 cells. In fact, no significant changes in cellular morphology, including lysis, rounding, etc. were observed. To the contrary, the MLO-Y4 cells grew well on all the sintered glasses and they developed a morphology analogous to that of the corresponding cells grown on the CTRL−. The cellular growth on the new MgO and/or SrO modified glasses, especially on the BGMIX_Mg one, even surpassed that on the sintered 45S5 sample.

These outcomes are backed by the results of the viability test with NR uptake. As a matter of fact, the graph in Figure 8(a) shows that the NR uptake after 24 h of direct contact to the sintered glasses is comparable to CRTL−, which means that no significant decreases in lysosomal activity imputable to cytotoxic effects could be observed, since any alteration of the cell surface or the lysosomal membrane due to the action of xenobiotics is known to result in a decreased uptake and binding of NR [84].

The results of the XTT test of the MLO-Y4 cells cultured in eluates from the glasses are proposed in Figure 8(b). XTT is a valuable micro-culture tetrazolium assay, since XTT involves the development of soluble formazans, which makes superfluous the error-prone solubilization step required in similar tests, such as MTT. In fact, MTT results in an insoluble formazan compound which requires dissolving the dye in order to measure it. Eliminating the final solubilization step means less manipulation and thus reduced risk of error [85]. The XTT results in Figure 8(b) show that none of the sintered glasses affected negatively the vitality of the cells; in particular, the MgO and/or SrO modified glasses exceeded the 45S5 reference, with a remarkably good outcome for BGMIX_Mg.

According to the BrdU test results in Figure 8(c), the sintered glasses did not interact negatively with the cell proliferation. Once more, the best results were achieved by the BGMIX_Mg sample, which surpassed by far the 45S5 sintered reference.

4. Conclusions

A CaO-rich, K_2O-containing silicate bioglass (BG_Ca-Mix, in mol%: 2.3 Na_2O; 2.3 K_2O; 45.6 CaO; 2.6 P_2O_5; 47.2 SiO_2) was modified by introducing MgO and/or SrO in fixed amounts in order to investigate the effect of such oxides, commonly present in human bone tissue, on the thermal behaviour, mechanical properties and bioactivity after sintering. In more detail, a fixed 10 mol% of CaO was replaced with MgO (BGMIX_Mg glass) or SrO (BGMIX_Sr) or fifty-fifty MgO-SrO (BGMIX_MgSr). In the modified glasses, the thermal behavior was governed both by the magnesium oxide/strontium oxide ratio and by the specific glass composition. Basically, the presence of MgO and/or SrO didn't interfere with the thermal stability of the parent glass, since all the new glasses could be sintered without any devitrification at relatively low temperatures, close to 750°C (sintering temperature: 753 °C for BGMIX_Mg; 750 °C for BGMIX_Sr; 759 °C for BGMIX_MgSr). This derives from the high crystallization temperatures of the modified glasses (peak crystallization temperature: 876 °C for BGMIX_Mg; 865 °C for BGMIX_Sr; 883 °C for BGMIX_MgSr), which systematically exceeded the corresponding sintering temperatures. Moreover the sintered glasses showed a strong volume shrinkage, from 11.97±0.89 % for BGMIX_MgSr up to 14.37±0.69 for BGMIX_Mg. The very limited residual porosity resulted in good mechanical properties, with a Young's modulus that ranged between 57.9 ± 6.7 GPa for BGMIX_MgSr and 112.6 ± 8.0 GPa for BGMIX_Mg. Besides a pronounced apatite-forming ability in a simulated body fluid (SBF), all the sintered glasses, tested with MLO-Y4 osteocytes by means of a multi-parametrical approach, showed a good bioactivity *in vitro*, since the samples themselves and their extracts did not cause any negative effect on cell viability and they didn't inhibit cell growth. To the contrary, the MgO-modified glasses, BGMIX_MgSr and especially BGMIX_Mg, were able to exert a particularly strong stimulating effect on cell growth, even superior to that of the sintered BG_Ca-Mix parent glass and the sintered 45S5 reference sample, thus proving to be optimal candidates for the fabrication of bioactive scaffolds and other sintered biomedical devices for dental implants and bone regeneration. To conclude, the partial replacement of CaO with MgO and/or SrO

preserves the strong sintering ability and limited tendency to crystallize of the parent glass, but the presence of such oxides, especially MgO, further improves the bioactivity.

5. References

1. V.J. Shirtliff, L.L. Hench, Bioactive materials for tissue engineering, regeneration and repair, J. Mater. Sci. 38 (2003) 4697-4707.
2. L.L. Hench, Bioceramics: from concept to clinic, J. Am. Ceram. Soc. 81 (1998) 1705-1728.
3. I.D. Xynos, M.V.J. Hukkanen, J.J. Batten, L.D. Buttery, L.L. Hench, J.M. Polak, Bioglass 45S5 stimulates osteoblast turnover and enhances bone formation in vitro: implications and applications for bone tissue engineering, Calcified Tissue Int. 67 (2000) 321-329.
4. R.M. Day, Bioactive glass stimulates the secretion of angiogenic growth factors and angiogenesis in vitro, Tissue Eng. 11 (2005) 768-777].
5. L.L. Hench, Chronology of bioactive glass development and clinical applications, New Journal of Glass and Ceramics 3 (2013) 67-73.
6. O. Peitl, E.D. Zanotto, L. L. Hench, Highly bioactive P_2O_5-Na_2O-CaO-SiO_2 glass-ceramics, J. Non-Cryst. Solids 292 (2001) 115-126.
7. D.C. Clupper, L.L. Hench, Crystallization kinetics of tape cast bioactive glass 45S5, J. Non-Cryst. Solids 318 (2003) 43-4.
8. A.R. Boccaccini, Q. Chen, L. Lefebvre, L. Gremillard, J. Chevalier, Sintering, crystallisation and biodegradation behaviour of Bioglass®-derived glass–ceramics, Faraday Discuss. 136 (2007) 27-44.
9. L. Lefebvre, J. Chevalier, L. Gremillard, R. Zenati, G. Thollet, D. Bernache-Assolant, A. Govin, Structural transformations of bioactive glass 45S5 with thermal treatments, Acta Mater. 55 (2007) 3305.
10. L. Lefebvre, L. Gremillard, J. Chevalier, R. Zenati, D. Bernache-Assolant, Sintering behaviour of 45S5 bioactive glass, Acta Biomater. 4 (2008) 1894-1903.

11. O. Bretcanu, X. Chatzistavrou, K. Paraskevopoulos, R. Conradt, I. Thompsond, A.R. Boccaccini, Sintering and crystallisation of 45S5 Bioglass® powder, J. Eur. Ceram. Soc. 29 (2009) 3299-3306.
12. O. Peitl, G. P. La Torre, L.L. Hench, Effect of crystallization on apatite-layer formation of bioactive glass 45S5. J. Biomed. Mater. Res. 30 (1996) 509-14.
13. D. Bellucci, V. Cannillo, A. Sola, An overview of the effects of thermal processing on bioactive glasses, Sci. Sint. 42 (2010) 307-320.
14. D. Bellucci, V. Cannillo, A. Sola, A new potassium-based bioactive glass: Sintering behaviour and possible applications for bioceramic scaffolds. Ceram. International. 37 (2011) 145-157.
15. M.G.W. Lockyer, D. Holland, R. Dupree, NMR investigation of the structure of some bioactive and related glasses, J. Non-Cryst. Solids 188 (1995) 207-219.
16. A. Sola, D. Bellucci, M.G. Raucci, S. Zeppetelli, L. Ambrosio, V. Cannillo, Heat treatment of Na_2O-CaO-P_2O_5-SiO_2 bioactive glasses: Densification processes and postsintering bioactivity, J. Biomed. Mater. Res. A 100A (2012) 305-322.
17. D. Bellucci, V. Cannillo, A. Sola, Calcium and potassium addition to facilitate the sintering of bioactive glasses, Mater. Lett. 65 (2011) 1825-1827.
18. D. Bellucci, A. Sola, V. Cannillo, Low temperature sintering of innovative bioactive glasses, J. Am. Ceram. Soc. 95 (2012) 1313-1319.
19. D. Bellucci, V. Cannillo, G. Ciardelli, P. Gentile, A. Sola, Potassium based bioactive glass for bone tissue engineering. Ceram. International 36 (2010) 2449-2453.
20. A. Cattini, D. Bellucci, A. Sola, L. Pawłowski, V. Cannillo, Suspension plasma spraying of optimised functionally graded coatings of bioactive glass/hydroxyapatite, Surf. Coat. Tech. 236 (2013) 118-126.
21. D. Bellucci, A. Sola, A. Anesi, R. Salvatori, L. Chiarini, V. Cannillo, Bioactive glass/hydroxyapatite composites: Mechanical properties and biological evaluation, Mater. Sci. Eng. C 51 (2015) 196-205.

22. P. Gentile, D. Bellucci, A. Sola, C. Mattu, V. Cannillo, G. Ciardelli, Composite scaffolds for controlled drug release: Role of the polyurethane nanoparticles on the physical properties and cell behaviour, J. Mech. Behav. Biomed. 44 (2015) 53-60.
23. A. Hoppe, N.S. Güldal, A.R. Boccaccini, A review of the biological response to ionic dissolution products from bioactive glasses and glass-ceramics, Biomaterials 32 (2011) 2757-2774.
24. J. Soulié, J.M. Nedelec, E. Jallot, Influence of Mg doping on the early steps of physico-chemical reactivity of sol-gel derived bioactive glasses in biological medium. Phys. Chem. Chem. Phys. 11 (2009) 10473–10483.
25. A. Saboori, M. Rabiee, F. Moztarzadeh, M. Sheikhi, M. Tahriri, M. Karimi, Synthesis, characterization and in vitro bioactivity of sol-gel-derived SiO_2–CaO–P_2O_5–MgO bioglass, Mater. Sci. Eng. C 29 (2009) 335–340.
26. S. J. Watts, R. G. Hill, M. D. O'Donnell, R. V. Law, Influence of Magnesia on the Structure and Properties of Bioactive Glasses, J. Non-Cryst. Solids 356 (2010) 517–524.
27. R. K. Rude, M. Olerich, Magnesium Deficiency: Possible role in Osteoporosis Associated with Gluten-Sensitive Enteropathy, Osteoporosis Int. 6 (1996) 453–461.
28. M. Diba, F. Tapia, A. R. Boccaccini, Magnesium-Containing Bioactive Glasses for Biomedical Applications, Int. J. Appl. Glass Sci. 3 (2012) 221–253.
29. E. Gentleman, Y.C. Fredholm, G. Jell, N. Lotfibakhshaiesh, M.D. O'Donnell, R.G. Hill, M.M. Stevens, The effects of strontium-substituted bioactive glasses on osteoblasts and osteoclasts in vitro, Biomaterials 31 (2010) 3949–3956].
30. P. J. Marie, P. Ammann, G. Boivin, C. Rey, Mechanisms of action and therapeutic potential of strontium in bone. Calcif Tissue Int 69 (2001) 121-129.
31. P. J. Meunier, C. Roux, E. Seeman, S. Ortolani, J.E. Badurski, T. D. Spector, J. Cannata, A. Balogh, E. M. Lemmel, S. Pors-Nielsen, R. Rizzoli, H. K. Genant, J. Y. Reginster, The effects of strontium ranelate on the risk of vertebral fracture in women with postmenopausal osteoporosis, New Engl. J. Med. 350 (2004) 459–468.

32. D. Bellucci, A. Sola, I. Cacciotti, C. Bartoli, M. Gazzarri, A. Bianco, F. Chiellini, V. Cannillo, Mg- and/or Sr- doped Tricalcium phosphate/bioactive glass composites: synthesis, microstructure and biological responsiveness, Mater. Sci. Eng. C 42 (2014) 312-324.
33. D. Bellucci, A. Sola, V. Cannillo, Hydroxyapatite and Tricalcium Phosphate composites with bioactive glass as second phase: state of the art and current applications, J. Biomed. Mater. Res. A 2016; 104:1030-56.
34. C. Lara, M.J. Pascual, A. Durán, Glass-forming ability, sinterability and thermal properties in the systems RO–BaO–SiO_2 (R = Mg, Zn), J. Non-Cryst. Solids 348 (2004) 149–155.
35. D. Bellucci, F. Chiellini, G. Ciardelli, M. Gazzarri, P. Gentile, A. Sola, V. Cannillo, Processing and characterization of innovative scaffolds for bone tissue engineering, J. Mater. Sci. Mater. Med. 23 (2012) 1397-1409.
36. R. E. Chinn, Ch. 4 - Grinding and Polishing. In: Ceramography: Preparation and Analysis of Ceramic Microstructures (#06958G), ASM International (2002) 35-44.
37. G.D. Quinn, P.J. Patel, I. Lloyd, Effect of Loading Rate Upon Conventional Ceramic Microindentation Hardness, J. Res. Natl. Inst. Stand. 107 (2002) 299–306.
38. W.C. Oliver, G.M. Pharr, An improved technique for determining hardness and elastic modulus using load and displacement sensing indentation experiments, J. Mater. Res. 7 (1992) 1564–1583.
39. T. Kokubo, H. Takadama, How useful is SBF in predicting in vivo bone bioactivity?, Biomaterials 27 (2006) 2907–2915.
40. International Standard 10993–5, Biological evaluation of medical devices — part 5: tests for cytotoxicity: in vitro methods, 2009.
41. International Standard 10993–12, Biological evaluation of medical devices — part 12: sample preparation and reference materials, 2007.
42. N. Lotfibakhshaiesh, D.S. Brauer, R.G. Hill, Bioactive glass engineered coatings for Ti6Al4V alloys: Influence of strontium substitution for calcium on sintering behaviour, J. Non-Cryst. Solids 356 (2010) 2583–2590.

43. Y.C. Fredholm, N. Karpukhina, D. S. Brauer, J.R. Jones, R.V. Law, R.G. Hill, Influence of strontium for calcium substitution in bioactive glasses on degradation, ion release and apatite formation. J R Soc Interface. 9 (2012) 880–889.

44. Y.C. Fredholm, N. Karpukhina, R.V. Law, R.G. Hill, Strontium containing bioactive glasses: glass structure and physical properties. J. Non-Crystal. Solids 356 (2010) 2546–2551.

45. E. Verné, O. Bretcanu, C. Balagna, C.L. Bianchi, M. Cannas, S. Gatti, C. Vitale-Brovarone, Early Stage Reactivity and In Vitro Behavior of Silica-Based Bioactive Glasses and Glass-Ceramics, J. Mater. Sci. Mater. Med 20 (2009) 75–87.

46. H.R. Swift, Effect of magnesia and alumina on rate of crystal growth in some soda-lime-silica glasses, J. Am. Ceram. Soc. 30 (1947) 170-174.

47. J. Ma, C. Z. Chen, D. G. Wang, Y. Jiao, J. Z. Shi, Effect of Magnesia on the Degradability and Bioactivity of Sol-Gel Derived SiO2–CaO–MgO–P2O5 System Glasses. Colloids Surf. B 81 (2010) 87–95.

48. J. Ma, C. Z. Chen, D. G. Wang, X. G. Meng, J. Z. Shi, In Vitro Degradability and Bioactivity of Mesoporous CaO-MgO-P(2)O(5)-SiO(2) Glasses Synthesized by Sol-Gel Method. J. Sol-Gel. Sci. Technol. 54 (2010) 69–76.

49. K. Shimoda, Y. Tobu, H. Hatakeyama, T. Nemoto, K. Saito, Structural Investigation of Mg Local Environments in Silicate Glasses by Ultra-High Field Mg-25 3QMAS NMR Spectroscopy, Am. Mineral. 92 (2007) 695–698.

50. A.M. George, J.F. Stebbins, Structure and Dynamics of Magnesium in Silicate Melts: A High-Temperature Mg-25 NMR Study. Am. Mineral. 83 (1998) 1022–1029.

51. A. Goel, S. Kapoor, R.R. Rajagopal, M.J. Pascual, H.-W. Kim, J.M.F. Ferreira, Alkali-free bioactive glasses for bone tissue engineering: A preliminary investigation, Acta Biomater. 8 (2012) 361–372.

52. D. Bellucci, A. Sola, V. Cannillo, Bioactive glass-based composites for the production of dense sintered bodies and porous scaffolds, Mater. Sci. Eng. C 33 (2013) 2138–2151.

53. A. Kozmidis-Petrovic, J. Šesták, Forty years of the Hrubÿ glass-forming coefficient via DTA when comparing other criteria in relation to the glass stability and vitrification ability, J. Therm. Anal. Calorim. 110 (2012) 997–1004.

54. C.A. Simmons, N. Valiquette, R.M. Pilliar, Osseointegration of sintered porous-surfaced and plasma spray-coated implants: An animal model study of early postimplantation healing response and mechanical stability. J. Biomed. Mater. Res. 47 (1999) 127-38.

55. K.A. Hing, B. Annaz, S. Saeed, P.A. Revell, T. Buckland, Microporosity enhances bioactivity of synthetic bone graft substitutes. J. Mater. Sci. Mater. Med. 16 (2005) 467-75.

56. X. Liu, C. Ding, P.K. Chu, Mechanism of apatite formation on wollastonite coatings in simulated body fluids, Biomaterials 25 (2004) 1755–1761.

57. K. Lin, W. Zhai, S. Ni, J. Chang, Y. Zeng, W. Qian, Study of the mechanical property and in vitro biocompatability of CaSiO3 ceramics. Ceram. Int. 31 (2005), 323–326.

58. P.N. De Aza, Z. Luklinska, M.R. Anseau, F. Guitian, S De Aza, Morphological studies of pseudowollastonite for biomedical application, J. Microsc. 182 (1996) 24–31.

59. G. Kaur, G. Pickrell, V. Kumar, O.P. Pandey, K. Singh, S.K. Arya, Mechanical, dielectric and optical assessment of glass composites prepared using milling technique, B. Mater. Sci. 38 (2015) 1003-1008.

60. V. Cannillo, L. Esposito, E. Rambaldi, A. Sola, A. Tucci, Effect of porosity on the elastic properties of porcelainized stoneware tiles by a multi-layered model, Ceram. Int. 35 (2009) 205–211.

61. L. Desogus, A. Cuccu, S. Montinaro, R. Orrù, G. Cao, D. Bellucci, A. Sola, V. Cannillo, Classical Bioglass® and innovative CaO-rich bioglass powders processed by Spark Plasma Sintering: A comparative study, J. Eur. Ceram. Soc. 35 (2015) 4277–4285.

62. T. Albrektsson, C. Johansson, Osteoinduction, osteoconduction and osseointegration. Eur Spine J 10 (2001) S96-S101.

63. L.L. Hench, The story of Bioglass®, J. Mater. Sci. Mater. Med. 17 (2006) 967-978.
64. T. Kokubo, Bioactive glass ceramics: properties and applications, Biomaterials 12 (1991) 155-163.
65. M. Bohner, J. Lemaitre, Can bioactivity be tested in vitro with SBF solution?, Biomaterials 30 (2009) 2175-2179.
66. D. Bellucci, A. Sola, R. Salvatori, A. Anesi, L. Chiarini, V. Cannillo, Sol-gel derived bioactive glasses with low tendency to crystallize: Synthesis, post-sintering bioactivity and possible application for the production of porous scaffolds. Mater Sci Eng C 43 (2014) 573-586.
67. S.V. Dorozhkin, Calcium orthophosphates in nature, biology and medicine, Materials 2 (2009) 399-498].
68. C. Vitale Brovarone, E. Verné, P. Appendino, Macroporous bioactive glass-ceramic scaffolds for tissue engineering, J. Mater. Sci. Mater. Med. 17 (2006) 1069–1078.
69. D. Bellucci, G. Bolelli, V. Cannillo, A. Cattini, Sola A, In situ Raman spectroscopy investigation of bioactive glass reactivity: simulated body fluid solution vs TRIS buffered solution, Mater. Charact. 62 (2011) 1021–1028.
70. D. Bellucci, A. Sola, P. Gentile, G. Ciardelli, V. Cannillo, Biomimetic coating on bioactive glass-derived scaffolds mimicking bone tissue, J. Biomed. Mater. Res. A 100 A (2012) 3259-3266.
71. G. Penel, G. Leroy, C. Rey, E. Bres, MicroRaman spectral study of the PO4 and CO3 vibrational modes in synthetic and biological apatite, Calcif. Tissue. Int. 63 (1998) 475–481.
72. A. Awonusi, M.D. Morris, M.M.J. Tecklenburg, Carbonate assignment and calibration in the Raman spectrum of apatite, Calcif. Tissue Int. 81 (2007) 46–52.
73. W. Paul, C.P. Sharma, Effect of calcium, zinc and magnesium on the attachment and spreading of osteoblast like cells onto ceramic matrices, J. Mater. Sci. Mater. Med. 18 (2007) 699–703.

74. E. Bonnelye, A. Chabadel, F. Saltel, P. Jurdic, Dual effect of strontium ranelate: stimulation of osteoblast differentiation and inhibition of osteoclast formation and resorption in vitro, Bone 42 (2008) 129–138.

75. S. Kotani, Y. Fujita, T. Kitsugi, T. Nakamura, T. Yamamuro, C. Ohtsuki, T. Kokubo, Bone bonding mechanism of β-tricalcium phosphate, J. Biomed. Mater. Res. 25 (1991) 1303–1315.

76. K. Ohura, M. Bohner, P. Hardouin, J. Lemaitre, G. Pasquier, B. Flautre, Resorption of, and bone formation from, new beta-tricalcium phosphate-monocalcium phosphate cements: an in vivo study, J. Biomed. Mater. Res. 30 (1996) 193–200.

77. W.R. Walsh, P. Morberg, Y. Yu, J.L. Yang, W. Haggard, P.C. Sheath, M. Svehla, W.J. Bruce, Response of a calcium sulfate bone graft substitute in a confined cancellous defect, Clin. Orthop. Relat. R. 406 (2003) 228–236.

78. F. Theiss, D. Apelt, B. Brand, A. Kutter, K. Zlinszky, M. Bohner, S. Matter, C. Frei, J.A. Auer, B. von Rechenberg, Biocompatibility and resorption of a brushite calcium phosphate cement, Biomaterials 26 (2005) 4383–4394.

79. H. Pan, X. Zhao, B.W. Darvell, W.W. Lu, Apatite-formation ability — predictor of "bioactivity"? Acta Biomater. 6 (2010) 4181–4188.

80. S.K. Bhatia, A.B. Yetter, Correlation of visual in vitro cytotoxicity ratings of biomaterials with quantitative in vitro cell viability measurements, Cell Biol. Toxicol. 24 (2008) 315–319.

81. Y. Kato, J.J. Windle, B.A. Koop, G.R. Mundy, L.F. Bonewald, Establishment of an osteocyte-like cell line. MLO-Y4, J. Bone Miner. Res. 12 (1997) 2014–2023.

82. L.F. Bonewald, Establishment and characterization of an osteocyte-like cell line, MLO-Y4, J. Bone Miner. Metab. 17 (1999) 61–65.

83. I. Kalajzic, B.G. Matthews, E. Torreggiani, M.A. Harris, P. Divieti Pajevic, S.E. Harris, In vitro and in vivo approaches to study osteocyte biology, Bone 54 (2013) 296–306.

84. E. Borenfreund, J.A. Puerner, A simple quantitative procedure using monolayer culture for toxicity assays, Journal of Tissue Culture Methods 9 (1984) 7–9.

85. C.J. Goodwin, S.J. Holt, S. Downes, N.J. Marshall, Microculture tetrazolium assays: a comparison between two new tetrazolium salts, XTT and MTS, J. Immunol. Methods 179 (1995) 95–103.

Figure captions

Figure 1. DTA curves of BGMIX_MgSr, BGMIX_Sr and BGMIX_Mg.

Figure 2. Cross sections of the BGMIX_Mg (a), BGMIX_Sr (b) and BGMIX_MgSr (c) samples treated at T_s (see Table 2 for specific temperatures) for 3 hours.

Figure 3. XRD spectra of the samples after specific thermal treatments for 3 hours. BGMIX_Mg samples were sintered at the final temperatures T = 876 °C and T = 1000 °C; BGMIX_Sr and BGMIX_MgSr were sintered at the final temperature T = 1000 °C.

Figure 4. HA formed on the surfaces of the BGMIX_Mg samples after 1 day (a), 3 days (b), 7 days (c) and 14 days (d) in SBF.

Figure 5. XRD spectra of a BGMIX_Mg sample soaked in SBF for increasing times

Figure 6. Raman spectra acquired on globular precipitates formed on the BGMIX_Mg surface after increasing soaking times in SBF; the inset reports an optical microscope image of the HA precipitates.

Figure 7. Morphological evaluation of MLO-Y4 cells after 24h direct contact with the samples using optical microscopy 10x magnification.

Figure 8. NR uptake after 24 h in the different glasses (a), XTT test of MLO-Y4 cells cultured in eluates from the glasses (b) and BrdU test of MLO-Y4 cells cultured in eluates from the different samples (c).

Table captions

Table 1. Compositions (in oxides mol%) of the produced glasses.

Table 2 Characteristic temperatures, sinterability parameter (S_c), Hruby parameter (K_H), volume shrinkage, Vickers hardness (HV) and Young's modulus (E_{it}) of the glasses.

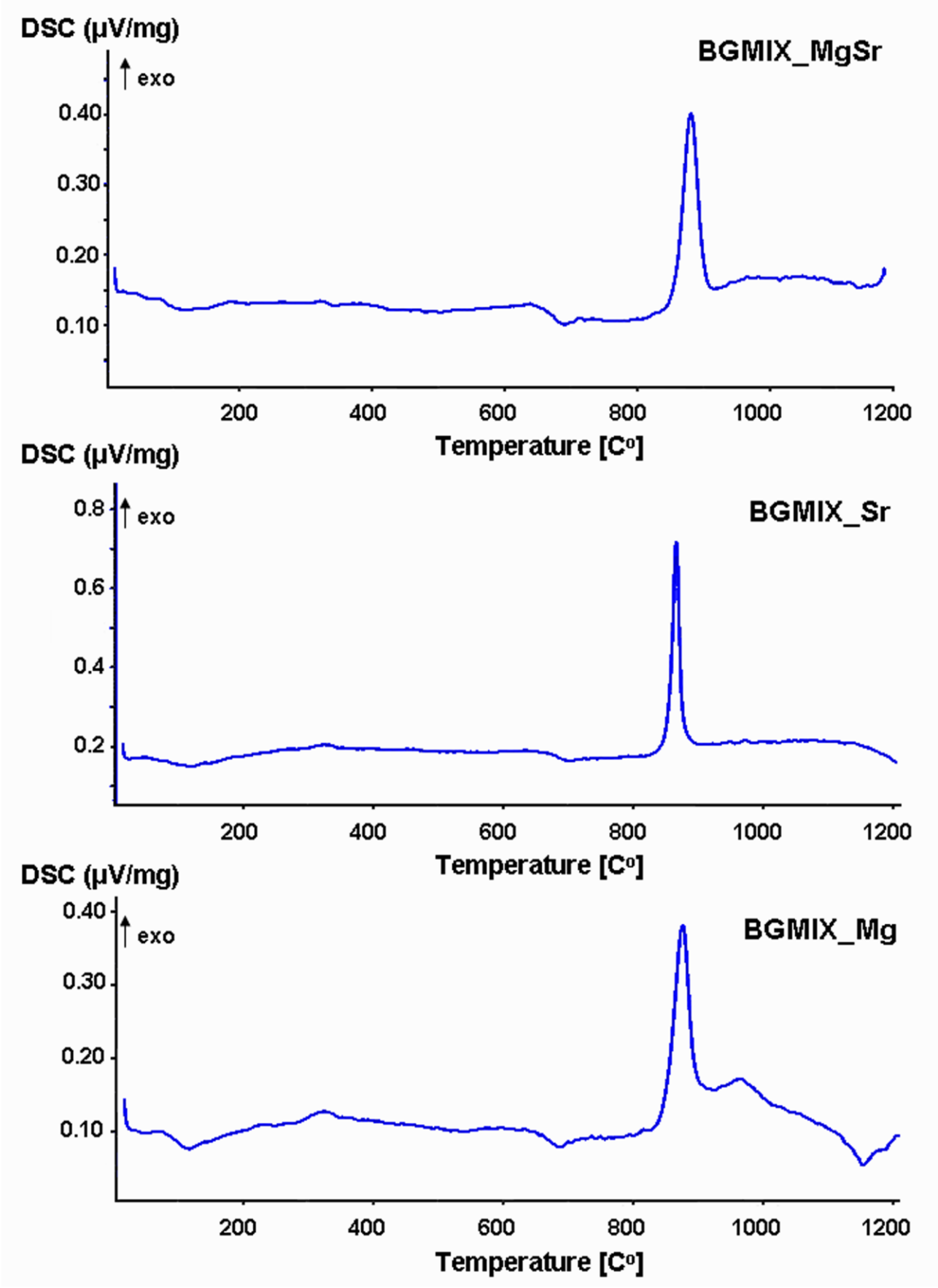

Fig. 1

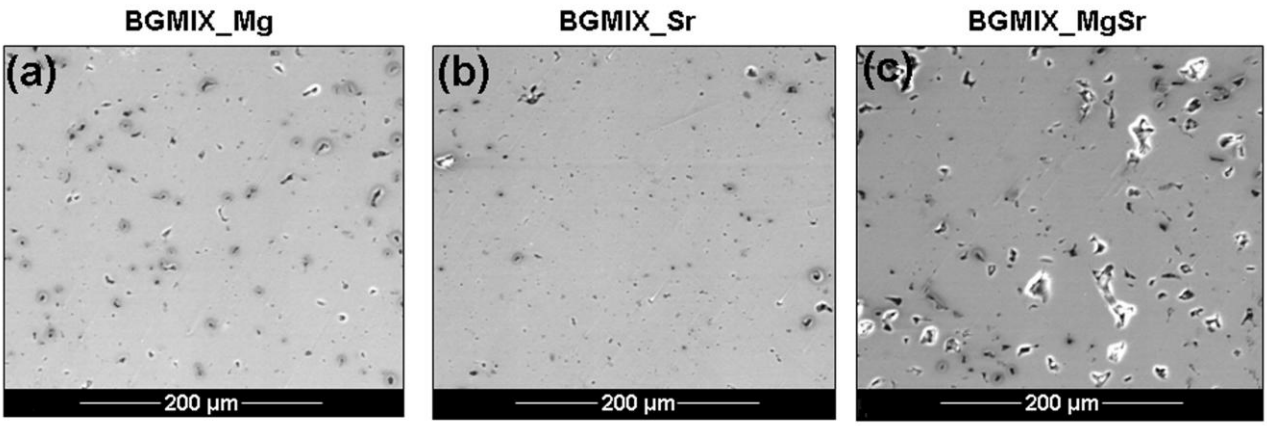

Fig. 2

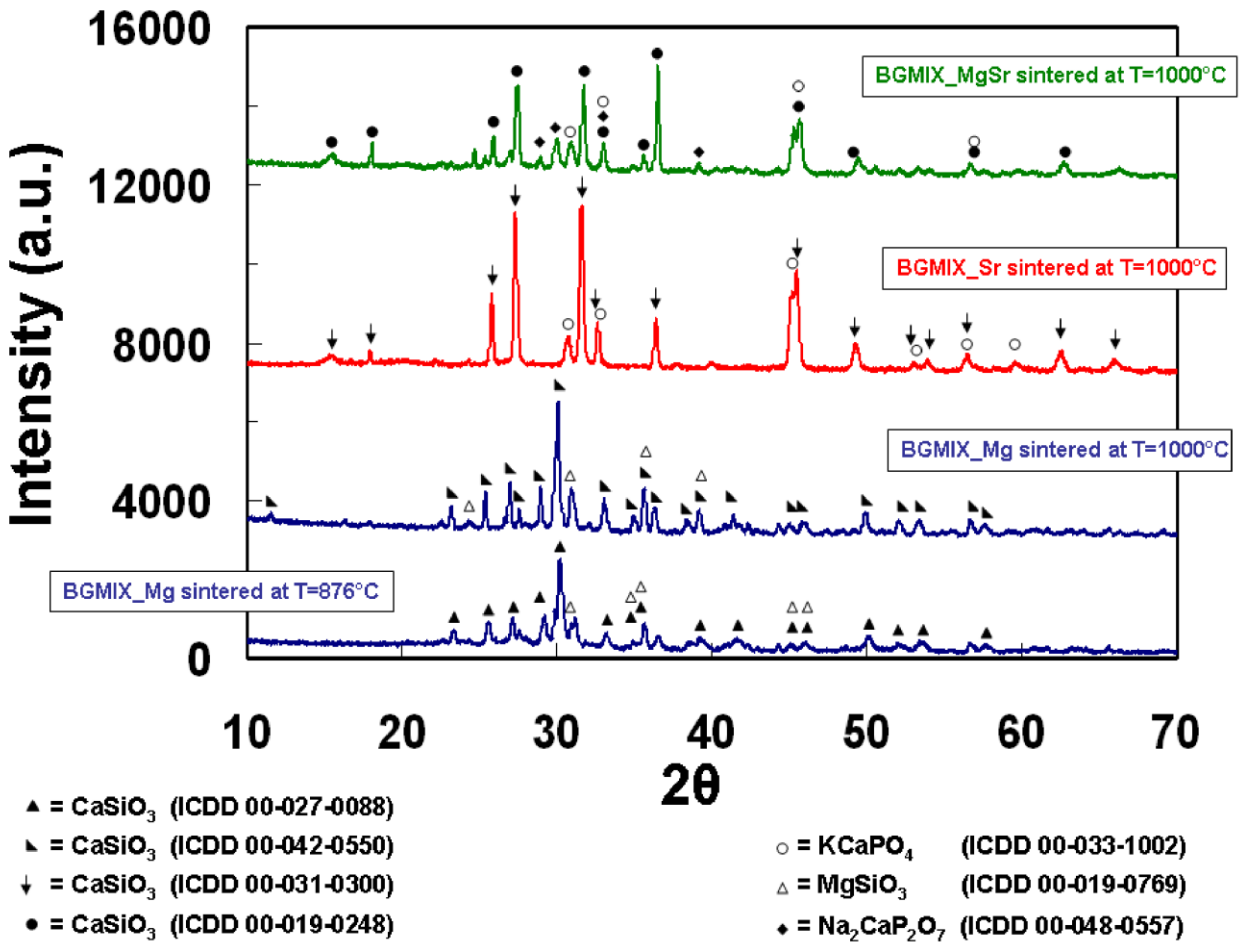

Fig. 3

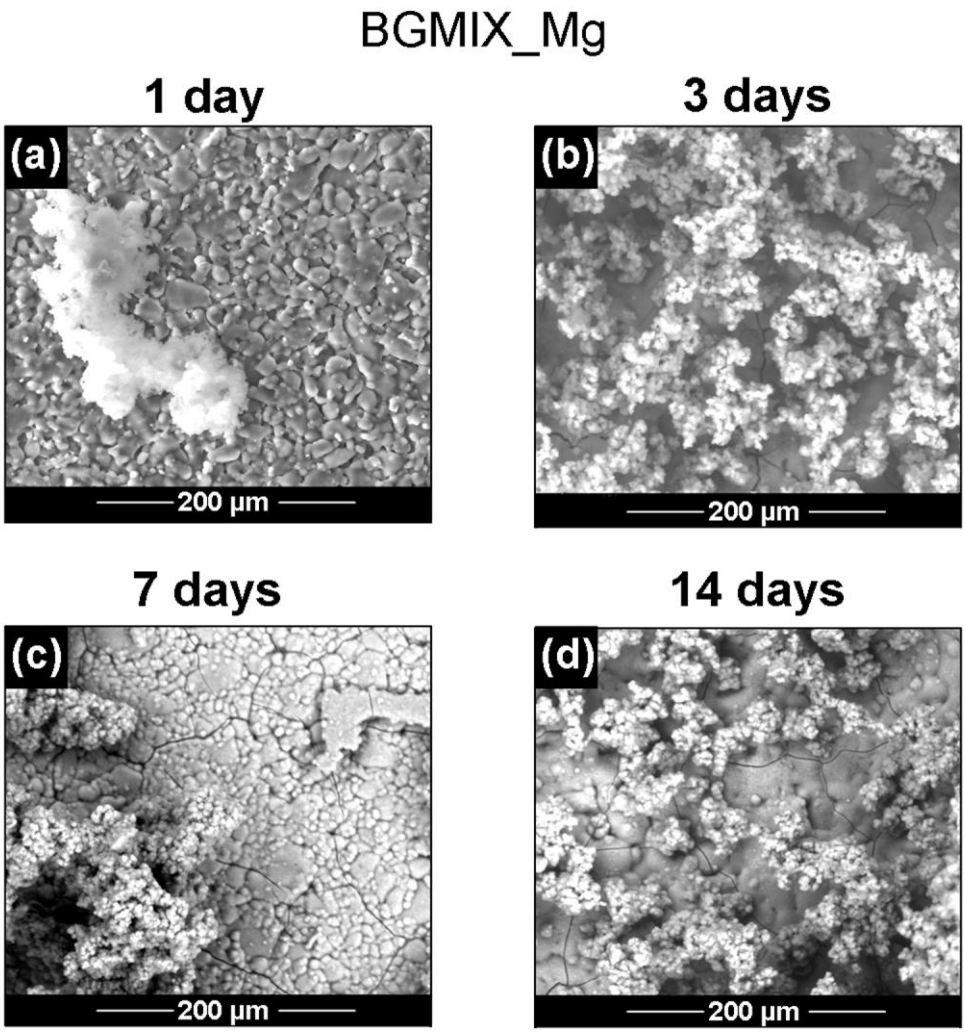

Fig. 4

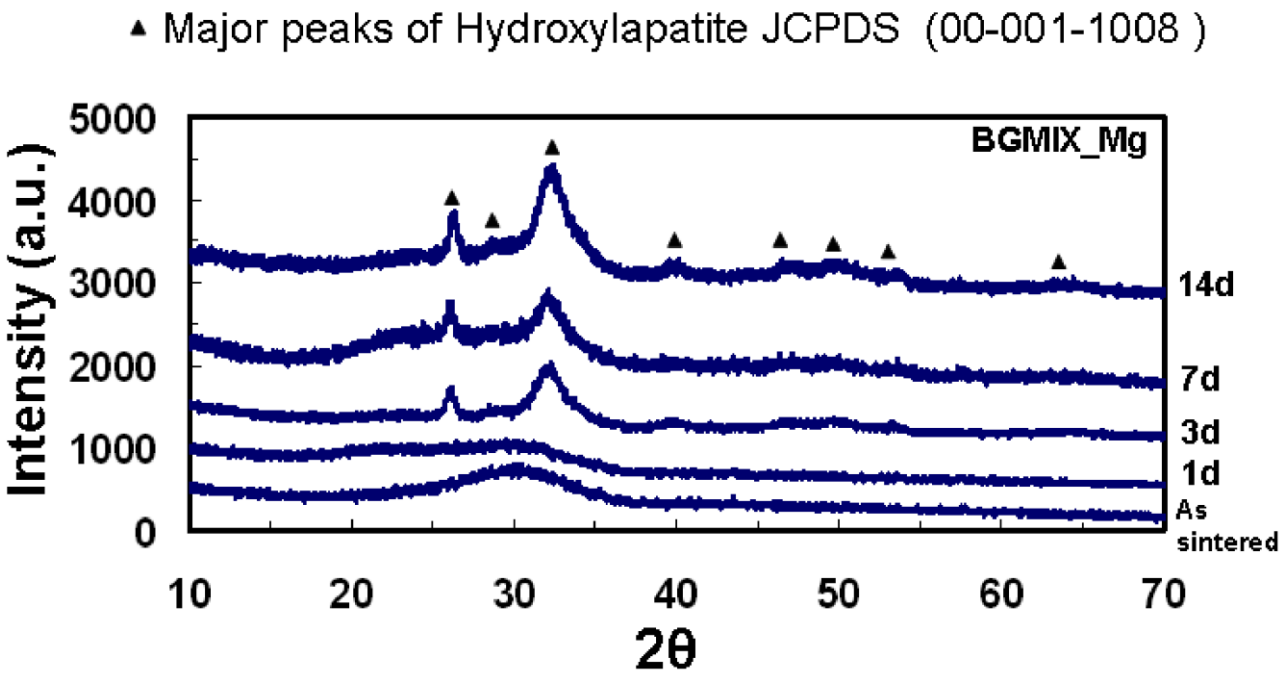

Fig. 5

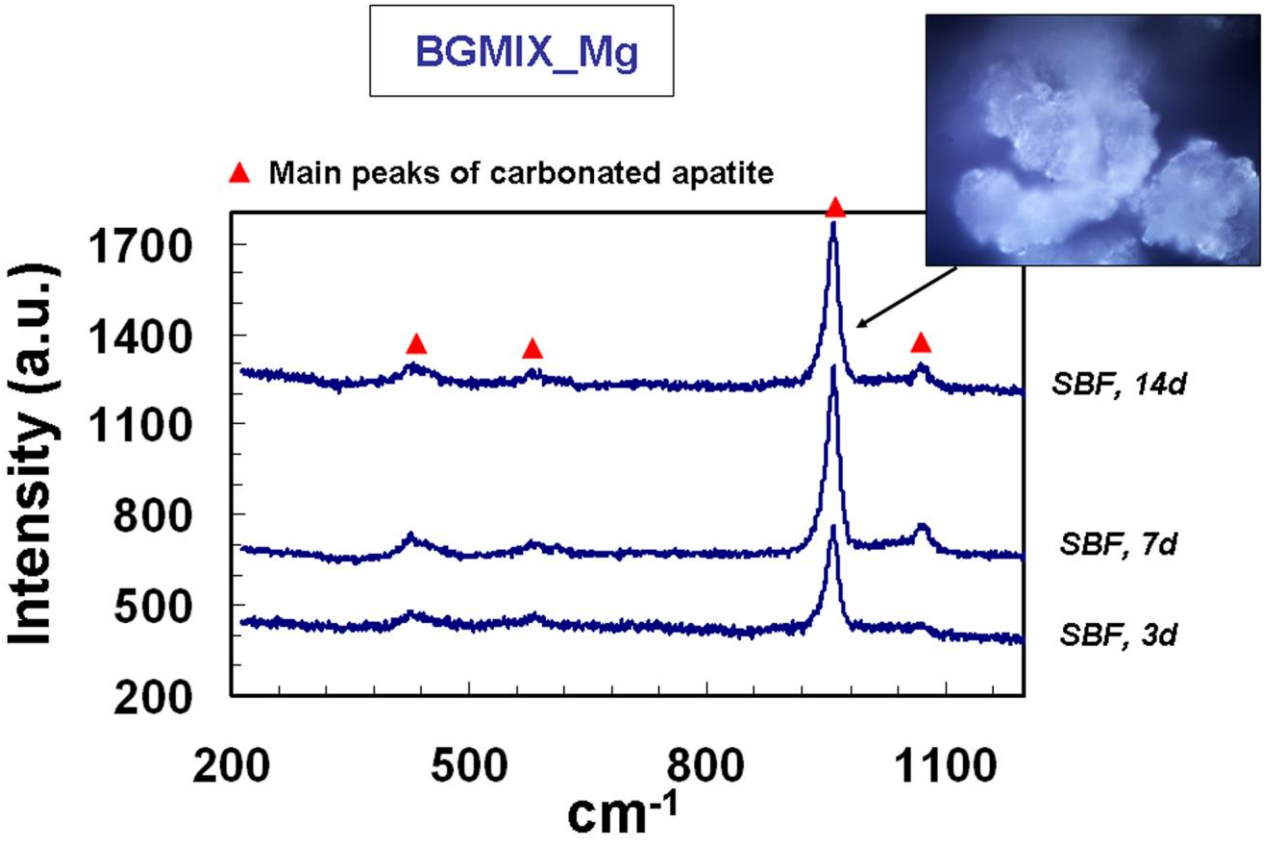

Fig. 6

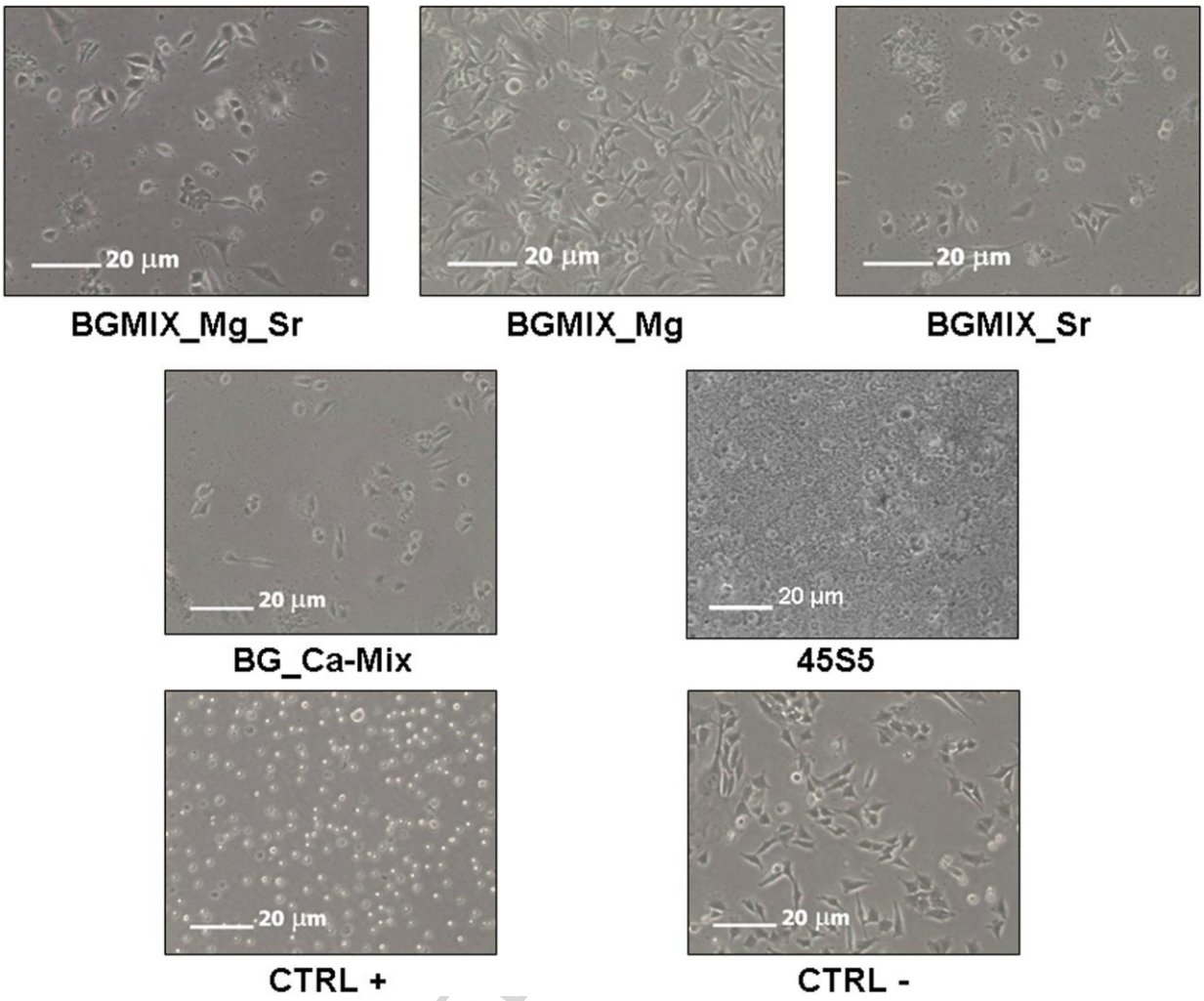

Fig. 7

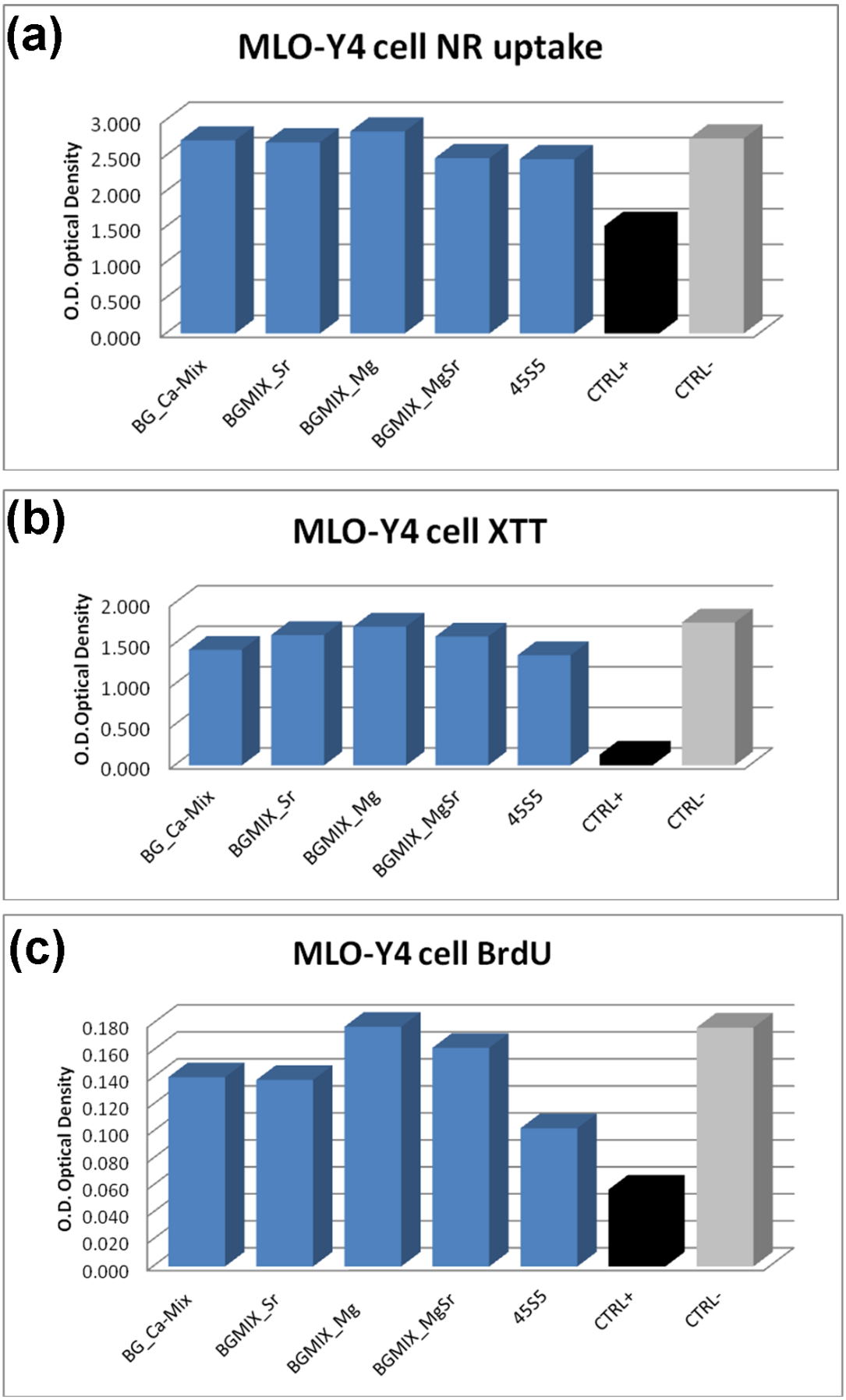
(a)
MLO-Y4 cell NR uptake
O.D. Optical Density
3.000
2.500
2.000
1.500
1.000
0.500
0.000
BG_Ca-Mix
BGMIX_Sr
BGMIX_Mg
BGMIX_MgSr
45S5
CTRL+
CTRL-
(b)
MLO-Y4 cell XTT
O.D.Optical Density
2.000
1.500
1.000
0.500
0.000
BG_Ca-Mix
BGMIX_Sr
BGMIX_Mg
BGMIX_MgSr
45S5
CTRL+
CTRL-
(c)
MLO-Y4 cell BrdU
O.D. Optical Density
0.180
0.160
0.140
0.120
0.100
0.080
0.060
0.040
0.020
0.000
BG_Ca-Mix
BGMIX_Sr
BGMIX_Mg
BGMIX_MgSr
45S5
CTRL+
CTRL-

Fig. 8

Oxides	**Composition [mol%]**			
	BG_Ca-Mix [18]	BGMIX_Mg	BGMIX_Sr	BGMIX_MgSr
SiO_2	47.2	47.2	47.2	47.2
P_2O_5	2.6	2.6	2.6	2.6
Na_2O	2.3	2.3	2.3	2.3
K_2O	2.3	2.3	2.3	2.3
CaO	45.6	35.6	35.6	35.6
MgO	0	10	0	5
SrO	0	0	10	5

Table 1. Compositions (in oxides mol%) of the produced glasses.

Sample Code	T_g (°C)	T_{c_onset} (°C)	T_c (°C)	T_m (°C)	T_s (°C)	S_c (°C)	K_H	Shrinkage (%)	HV (Vickers)	Eit (GPa)
BG_Ca-Mix [18]	720	860	880	1339	782	78	0.29	12.93±0.67	564 ± 47	65 to 122*
BGMIX_Mg	660	832	876	1214	753	79	0.45	14.37±0.69	448.4 ± 93.8	112.6 ± 8.0
BGMIX_Sr	675	838	865	1282	750	88	0.37	13.68±0.51	485.2 ± 28.0	93.6 ± 2.7
BGMIX_MgSr	655	841	883	1243	759	82	0.46	11.97±0.89	458.6 ± 91.2	57.9 ± 6.7

* values obtained for BG_Ca-Mix samples sintered by Spark Plasma Sintering under various processing conditions [61].

Table 2. Characteristic temperatures, sinterability parameter (S_c), Hruby parameter (K_H), volume shrinkage, Vickers hardness (HV) and Young's modulus (E_{it}) of the glasses.

Highlights

- The composition of a CaO-rich, K_2O-containing silicate bioglass was modified:
- A fixed 10 mol% of CaO was replaced with MgO or SrO or fifty-fifty MgO-SrO.
- The sintered glasses showed a strong volume shrinkage with low residual porosity;
- The samples showed good mechanical performance and apatite-forming ability in vitro;
- The presence of such oxides, especially MgO, improves the samples' bioactivity.